

## Self-Similar Structures near Boundaries in Strained Systems

B. Audoly\*

*Laboratoire de modélisation en mécanique, UMR 7607 du CNRS, Université Pierre et Marie Curie,  
4 place Jussieu, F-75252 Paris Cedex 05*

A. Boudaoud

*Laboratoire de Physique Statistique, UMR 8550 du CNRS, École normale supérieure, 24 rue Lhomond, F-75231 Paris Cedex 05  
(Received 8 April 2003; published 21 August 2003)*

We study the buckling of thin elastic plates caused by residual strains concentrated near a free edge. This is a model for plant leaves and torn plastic sheet morphologies. We derive new governing equations explaining self-similar patterns reported earlier in experiments. We reveal the cascade mechanism, determine the bounds for its wavelengths, and predict a similarity factor of 3 in agreement with experiments. This is confirmed by numerical solutions with up to five generations of wrinkles.

DOI: 10.1103/PhysRevLett.91.086105

PACS numbers: 68.55.-a, 46.32.+x

Self-similar structures are ubiquitous in nature. Examples range from snowflakes to turbulent flows. The complexity of such structures often prevents their full physical understanding: turbulence [1], for instance, is still the subject of numerous investigations. In some cases, self-similarity arises from minimization of the system energy, as in ferromagnetic materials [2,3] or in martensitic phase transitions [4]. In a recent paper [5], self-similar wrinkles were observed along the edge of torn plastic sheets and along the edge of plant leaves. Such plastic sheets exhibit a cascade of wrinkles with wave numbers  $k$ ,  $\alpha k$ ,  $\alpha^2 k$ ,  $\alpha^3 k$ , ..., with the self-similarity factor measured as  $\alpha \approx 3.2$ . Plastic flow near the crack tip or enhanced tissue growth near the leaf edge stretches a thin rectangular strip of material along the boundary. Wrinkling allows relaxation of the resulting strain [6]. This is reminiscent of the buckling of thin films under strong compression [7–9], although the physics turns out to be different (different energy scalings, role played by embeddings, ...). While the wrinkles observed in experiments are often self-similar [5], a precise account of such patterns based on the equations of elasticity is still lacking. Preliminary attempts based on the theory of elastic rods could account for wrinkling [10,11] but not for self-similarity. In this Letter, we address this problem starting from the full equations for elastic plates. We uncover the mechanism responsible for the cascade and fully characterize its self-similar structure: we predict  $\alpha = 3$  and determine the cutoff wavelengths. Our results are supported by numerical calculations showing up to five generations of wrinkles. Incidentally, we give a numerical answer to the existence of embeddings, an open problem in the differential geometry of surfaces [12]. We believe that the present work will extend to other systems where metric properties are important, as in general relativity, and where patterns follow from energy minimization.

In this Letter, we consider a thin elastic sheet with a stretched edge. In contrast to classical plates, its natural

configuration is described by a non-Euclidean 2D metric:

$$ds^2 = (1 + g(y))^2 dx^2 + dy^2, \quad (1)$$

where  $(x, y)$  are coordinates such that the stretched edge is at  $y = 0$  (Fig. 1). We use a Lagrangian description, as usual in elasticity, the reference state being parametrized by  $(x, y)$ . When  $g(y) \geq 0$  in Eq. (1), the reference planar configuration is in unstable equilibrium due to a compressive strain  $\epsilon_{xx} = -g(y)$ . The aim of the present work is to study relaxation of these stresses by buckling.

Such a metric accounts for stretched edges, as obtained in torn plastic sheets or in plant leaves. The form (1) of the metric is the most general one that is invariant along the edge direction  $x$  [13]. We shall not try to explicitly relate the metric profile  $g(y)$  to microscopic features (plasticity, cell growth) of these systems, but instead consider this model problem in its full generality and take  $g(y)$  as given. We shall retain only two physical features of  $g$ : it is negligible far away from the edge  $y = 0$  and varies over a small characteristic length. In torn plastic sheets, this small length scale comes from the regularization of divergent elastic stresses near the crack tip.

We derive the equations of elastic equilibrium for plates with a stretched edge by extending the classical theory [14] to account for  $g(y)$ . Deformations of thin plates can be decomposed into bending and stretching. Because of the small parameter  $h/R$ , the ratio of the thickness to the typical extent of the plate, bending costs much less energy than stretching, and purely flexural deformations are preferred. Such deformations may or may not exist depending on the form of  $g(y)$ . They exist provided one can find a surface in the usual 3D Euclidean space whose metric coincides with (1), as it yields a configuration with zero stretching energy. This geometrical question is classically referred to as finding (*isometric*) embeddings of an abstract manifold with metric (1) in  $\mathbb{R}^3$ .

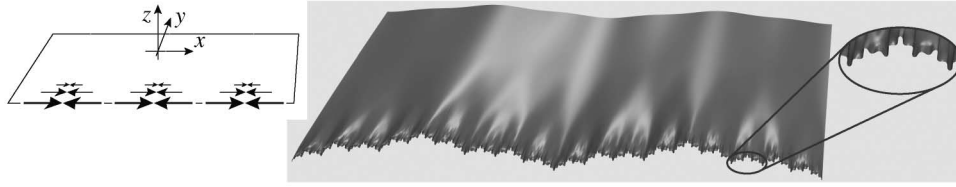


FIG. 1. An elastic plate buckles into a self-similar pattern due to residual strains near the edge (inset). Numerical solution for thickness  $h = 2.9 \times 10^{-5}$ , width 1, metric perturbation  $g(y) = 1/(1 + y/\ell)$ ,  $\ell = 0.008$ , yielding wavelength  $2\pi/k = 0.54$ .

Despite its simplicity, the existence of embeddings for arbitrary  $g(y)$  remains an open question [12]. As a result, one does not even know the structure of the lowest energy configurations of a sheet with a stretched edge, nor the order of magnitude of its elastic energy. We will give a numerical answer to this question and discuss in detail the structure of equilibrium configurations.

We first derive our plate model. Let  $u(x, y)$ ,  $v(x, y)$ , and  $\zeta(x, y)$  be, respectively, the  $x$ ,  $y$ , and  $z$  components of the displacement. In the small slope and small in-plane displacement approximations, the 2D strains of the mean

surface read  $\epsilon_{xx} = u_{,x} + \zeta_{,x}^2/2 - g(y)$ ,  $\epsilon_{yy} = v_{,y} + \zeta_{,y}^2/2$ , and  $\epsilon_{xy} = (u_{,y} + v_{,x} + \zeta_{,x}\zeta_{,y})/2$ , where  $f_{,x}$  stands for  $\partial f/\partial x$ . The Föppl–von Kármán (FvK) equations for plates are built upon this form of the strains [14] in the simpler particular case  $g(y) = 0$ . These equations have been the subject of renewed interest in the context of singularities [15–17]. Here, the presence of  $g(y)$  in  $\epsilon_{xx}$  favors configurations close to the natural metric (1) rather than developable ones as for classical plates.

For small  $g(y)$ , strains remain small and Hookean (linear) elasticity leads to the following energy [14]:

$$\mathcal{E} = \iint dx dy \left( \frac{Eh}{2(1-\nu^2)} [\nu(\epsilon_{xx} + \epsilon_{yy})^2 + (1-\nu)(\epsilon_{xx}^2 + 2\epsilon_{xy}^2 + \epsilon_{yy}^2)] + \frac{Eh^3}{24(1-\nu^2)} (\Delta\zeta)^2 \right), \quad (2)$$

where  $E$  and  $\nu$  are the Young's modulus and the Poisson ratio of the material. The first term in the integral is the stretching energy  $\mathcal{E}_s$  built upon the in-plane stresses given above while the second term is the bending energy.

We restrict our analysis to periodic solutions in the direction  $x$  parallel to the edge. The wave number  $k$  in this direction will later be selected by energy minimization. Fourier components are denoted using a superscript  $[q]$ , where the integer  $q$  tags the harmonic. Applying the Parseval formula to the stretching energy yields

$$\mathcal{E}_s = \frac{Eh}{2(1-\nu^2)} \int dy \sum_{qq'ii'jj'} \epsilon_{ij}^{[q]}(y) A_{ij,i'j'}^{q,q'} \epsilon_{i'j'}^{[q]}(y), \quad (3)$$

where the numbers  $A_{ij,i'j'}^{q,q'}$  were computed from Eq. (2). The bending energy in (2) was transformed similarly.

The equilibrium equations, obtained by variation with respect to  $u$ ,  $v$ , and  $\zeta$ , are not given here as they have no analytical solutions in general—even the simpler problem of finding an embedding, i.e., of solving  $\epsilon_{ij} = 0$  for

$i, j = x, y$ , has no general solution. Their numerical solution is also difficult because of the small parameter  $h/R$ , of the high order of derivation, and of the number of unknown functions ( $u, v, \zeta$ ).

To circumvent these difficulties, we introduce an approximation that leads to a fast numerical implementation of the buckling problem and allows for simpler analysis while leaving unchanged the salient features of the system. The elastic energy [stretching energy in Eq. (3) plus similar bending energy] is a quadratic form of the Fourier components  $\epsilon_{ij}^{[q]}(y)$  and  $\zeta^{[q]}(y)$ . Instead of minimizing the full quadratic form, we set to zero some suitably chosen components and minimize with respect to the remaining ones. We chose to set to zero the components  $\epsilon_{xx}^{[q]} = 0$  and  $\epsilon_{xy}^{[q]} = 0$  for  $q > 0$ , which yields  $u$  and  $v$  in terms of  $\zeta(x, y)$  directly: the benefit of the approximation, discussed at the end of this Letter, is that  $u$  and  $v$  can be eliminated from the energy functional (2), hence one unknown function remains instead of three. This leads to the following energy in terms of  $\zeta(x, y)$  only:

$$\mathcal{E} = \frac{Eh}{2(1-\nu^2)} \int dy \left[ \left( \left\langle \frac{1}{2} \zeta_{,x}^2 \right\rangle - g(y) \right)^2 + \frac{1}{2} \sum_{q>0} \left( \frac{\{\zeta_{,xx}\zeta_{,yy} - \zeta_{,xy}^2\}^{[q]}}{k^2 q^2} \right)^2 + \frac{h^2}{12} \langle (\Delta\zeta)^2 \rangle \right], \quad (4)$$

where brackets  $\langle f \rangle = f^{[0]}$  denote averages over  $x$ .

The stretching energy appearing in Eq. (4) has a simple geometric interpretation. Gauss's *theorema egregium* states that Gaussian curvature  $K$  is conserved by embeddings. In the limit  $|g| \ll 1$ , the Gaussian curvature associated with metric (1) is  $K(x, y) = -g''(y)$ , while for a profile  $\zeta(x, y)$ , it reads  $K(x, y) = \zeta_{,xx}\zeta_{,yy} - \zeta_{,xy}^2$ . Therefore,

no stretching  $\epsilon_{xx} = \epsilon_{yy} = \epsilon_{xy} = 0$  ( $\mathcal{E}_s = 0$ ) corresponds to  $\zeta_{,xx}\zeta_{,yy} - \zeta_{,xy}^2 = -g''(y)$ . The first Fourier component of this last equality integrated twice with respect to  $y$  yields  $\langle \zeta_{,x}^2/2 \rangle = g(y)$ , while any nonzero Fourier component  $q$  reads  $\{\zeta_{,xx}\zeta_{,yy} - \zeta_{,xy}^2\}^{[q]} = 0$ ; one recognizes the stretching terms in Eq. (4). This shows that our

stretching energy penalizes any deviation from an embedding and, conversely, that embeddings have no stretching energy. Our approximation scheme is specifically designed to respect embeddings in this sense and, to our knowledge, it is the first one having this key property.

The elastic energy (4) is invariant when  $g(y)$  and the other quantities  $[\zeta(x, y), h, \dots]$  are rescaled by an overall factor  $G: g(y) \mapsto g(y)/G, \zeta \mapsto \zeta/\sqrt{G}, \dots$ . This shows, surprisingly, that the self-similar solutions obtained below may exist for arbitrarily small perturbation  $g(y)$  of the flat metric, provided the plate is thin enough. In the following, the energy is minimized with respect to the fundamental wave number  $k$  and to the Fourier components  $\zeta^{[q]}(y)$  of the deflection ( $q = 0, 1, 2, \dots$ ). This minimization is based on 1D finite elements for the functions  $\zeta^{[q]}(y)$  ( $0 \leq q \leq q_{\max}$ ). The particular form of our energy leads to a very efficient implementation allowing interactive calculations and solution tracking (Figs. 3 and 4).

By numerical minimization of the elastic energy (4) we obtained self-similar solutions with up to five generations of wrinkles (Fig. 1). They were found to be absolute minima of energy when  $g(y)$  is peaked near  $y = 0$  with a small length scale there (see introduction). The cascade is generated by period tripling, and exhibits the wave numbers  $k, 3k, 9k, 27k$ , and  $81k$ . We now explain this period tripling using symmetries. The reflection invariance  $\zeta \mapsto -\zeta$  in the plate Eq. (4) leads to the coupling of *odd* Fourier components  $\zeta^{[q]}(y)$  only. As a result, the self-similarity factor  $\alpha$  must map odd integers to odd integers: this leaves only odd integers ( $\alpha = 3, 5$ , etc.) as eligible values. Our simulation shows that  $\alpha = 3$  yields the lowest energy, although solutions for  $\alpha = 5$  do not cost much more. This compares well with the experimental  $\alpha \approx 3.2$  reported in Ref. [5]. The slight discrepancy can be attributed to experimental nonlinearities of the order of 1 while  $|g| \ll 1$  here. Moreover, a factor  $\alpha$  close to 5 has indeed been observed in some experiments [18].

From the form of the stretching energy in Eq. (4), self-similar solutions are invariant under the transform:

$$\bar{x} = 3x, \quad \bar{y} = 3y, \quad \bar{q} = q/3, \quad \frac{\bar{q}\zeta^{[\bar{q}]}(\bar{y})}{\sqrt{g(\bar{y})}} = \frac{q\zeta^{[q]}(y)}{\sqrt{g(y)}}, \quad (5)$$

where we restrict our analysis to the case  $\alpha = 3$ . This invariance is confirmed by the collapse of numerical functions  $\zeta^{[q]}(y)$  (Fig. 2). Note that the fixed-point function of the collapse is not universal and depends on  $g(y)$ .

The order of magnitude of the fundamental wave number  $k$  is given by the macroscopic extent of the plate (its width in our simulations and in experiments). This gives the largest wavelength of the solution. Its smallest wavelength is determined by a mechanism analyzed below. The cascade takes place over all intermediate scales by successive period tripling.

Regularization of the wrinkles at very small scales is due to bending effects, which penalize short scale oscillations. Let  $\lambda$  be the smallest wrinkling wavelength, and

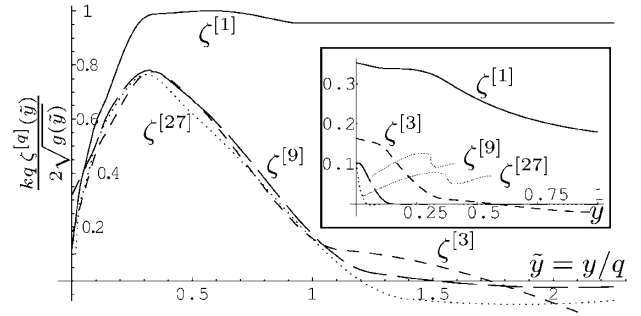


FIG. 2. Fourier components  $\zeta^{[q]}(y)$  ( $q = 1, 3, 9, 27$ ) of the deflection for a numerical self-similar solution with four generations (inset) and their collapse using transform (5).  $\zeta^{[1]}(y)$  need not collapse away from the stretched edge (i.e., large  $y$ ). Same parameters as in Fig. 1, except for  $h = 2.9 \times 10^{-4}$ .

$\ell = |g(0)/g'(0)|$  be the small length scale induced by  $g(y)$  near the edge. The cutoff  $\lambda$  is found by balancing stretching and bending energies at scale  $\lambda$ . For the metric used in the simulations of Fig. 3, this yields  $\lambda \sim h^{2/5}\ell^{3/5}$ , in agreement with the numerics. Incidentally, this formula shows that a cascade requires a small scale  $\ell$  in the metric: if  $\ell$  is too large, only one wavelength is present.

Our plate model and its numerical implementation provide insights into the physical structure of the self-similar solutions. Earlier papers suggested that the mechanism responsible for the cascade is essentially geometric [5,6]: embeddings with a single wavelength would disappear when  $\ell$  becomes small enough and be replaced by embeddings made of wrinkles with many wavelengths. According to this scenario, the bifurcation would take place for purely geometrical reasons. In direct contrast, we show below that self-similar solutions are selected by flexural effects: the interplay between elasticity and geometry is essential.

To demonstrate this, we considered a one-parameter family of functions  $g_\ell(y)$ , and tracked solutions minimizing the total elastic energy while  $\ell$  was varied. As shown in Fig. 4, when the small length scale  $\ell$  is decreased, the

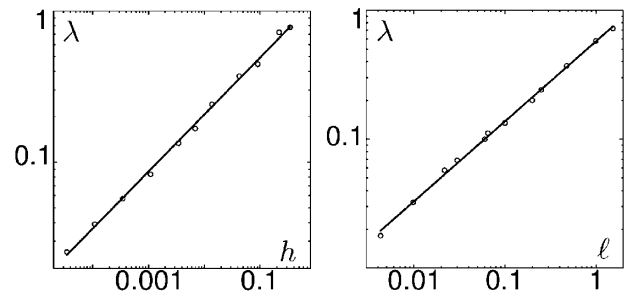


FIG. 3. Numerical check of scaling law  $\lambda \sim h^{2/5}\ell^{3/5}$ : smallest wavelength  $\lambda$  in the cascade versus plate thickness  $h$  (left panel) and metric typical length  $\ell$  (right panel) for the family of metric perturbations  $g_\ell(y) = 1/(1 + y/\ell)$ . Thick lines are best power-law fits, yielding exponents 0.38 and 0.62, respectively.

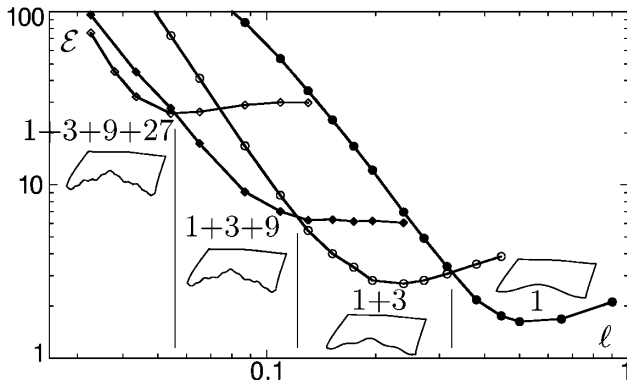


FIG. 4. Total elastic energy of solutions with one to four generations of wrinkles for the one-parameter family of metrics  $g_\ell(y) = 1/(1 + y/\ell)$ . Unit of energy is the bending modulus [i.e., the prefactor of the bending energy in Eq. (2)]. Bifurcations occur while all branches remain close to embeddings: they are selected by minimization of bending energy.

lowest energy configuration bifurcates from a single wavelength (“1”) to a cascade of wrinkles by successive period tripling (up to “1 + 3 + 9 + 27”). Remarkably, all these configurations were found numerically to converge to embeddings in the limit  $h \rightarrow 0$  [19]. This shows that, for a given  $g_\ell(y)$ , there exist *many* embeddings, one of which is made up of oscillations at a single length scale while others are a superposition of wrinkles with many wavelengths. This rules out the possibility of a merely geometrical selection. Among these several embeddings, self-similar configurations are selected because their bending energy is smaller. Indeed, near the edge, the curvature along the  $x$  direction is of the order of  $\zeta/\lambda^2$ , while that along  $y$  is of the order of  $\zeta/\ell^2$ . To minimize stretching, the boundary almost has its natural length, hence  $\zeta \sim \lambda\sqrt{g(0)}$ . The density of bending energy  $Eh^3g(0)(1/\lambda + \lambda/\ell^2)^2$  is therefore minimum when  $\lambda \sim \ell$ . Qualitatively, this means that small wavelengths are favored near the boundary, hence the cascade.

This mechanism and all the main findings of this Letter are robust with respect to the approximations used to derive our plate energy (4). The small slope approximation in our definition of strains (as in the FvK equations) is justified by our finding of self-similar solutions for small  $g(y)$ , hence for small strains and slopes. Concerning the additional constraints put on some of the strain components to simplify the form of the energy functional, we stress that (i) this approximation respects embeddings, thereby avoiding overestimation of the energy by a large factor [8], a difficulty that can arise in poorer approximation schemes; (ii) that for some particular configurations we have relaxed these constraints and resorted to the classical FvK equations without observing qualitative changes in the resulting patterns, but at the price of a much higher CPU usage; (iii) that our main findings summarized below are robust and still hold for the full FvK equations, as can be checked directly.

We have explained the formation of self-similar wrinkles in elastic plates with a stretched edge as follows. In a first (geometrical) step, configurations are restricted to embeddings to avoid a strong penalization by the stretching energy; this problem is degenerate: many profiles are possible, as shown numerically. In a second (elastic) step, self-similar wrinkles are selected due to the presence of a small characteristic length  $\ell$  near the edge. The invariant magnification factor  $\alpha = 3$  was predicted, in agreement with experiments. The bounds for the wavelengths present in the cascade were determined. Unexpectedly, self-similar patterns can be found for arbitrarily small  $g(y)$  ( $G$  invariance), so that the cascade is not due to strong nonlinearities. We have pointed out a new mechanism by which the underlying non-Euclidean metric properties of a physical system generates self-similar patterns.

We would like to thank K. R. Min for presenting us her experiments and M. Marder, B. Roman, and E. Sharon for fruitful discussions.

\*URL: <http://www.lmm.jussieu.fr/~audoly/>

- [1] B. B. Mandelbrot, *J. Fluid Mech.* **72**, 401 (1975).
- [2] R. Choksi, R. V. Kohn, and F. Otto, *Commun. Math. Phys.* **201**, 61 (1999).
- [3] E. M. Lifshitz, *J. Phys. (Paris)* **8**, 337346 (1944).
- [4] S. Conti, *Commun. Pure Appl. Math.* **53**, 1448 (2000).
- [5] E. Sharon, B. Roman, M. Marder, G. S. Shin, and H. L. Swinney, *Nature (London)* **419**, 579 (2002).
- [6] S. Nechaev and R. Voiturier, *J. Phys. A* **34**, 11069 (2001).
- [7] Y. Pomeau and S. Rica, *C.R. Acad. Sci. Paris Ser. II* **325**, 181 (1997).
- [8] W. Jin and P. Sternberg, *J. Math. Phys. (N.Y.)* **42**, 192 (2001).
- [9] H. B. Belgacem, S. Conti, A. DeSimone, and S. Müller, *Arch. Ration. Mech. Anal.* **164**, 1 (2002).
- [10] B. Audoly and A. Boudaoud, *C.R. Mecanique* **330**, 831 (2002).
- [11] M. Marder, E. Sharon, B. Roman, and S. Smith, *Europhys. Lett.* **62**, 498 (2003).
- [12] M. Spivak, *Differential Geometry* (Publish or Perish Inc., Berkeley, CA, 1979), Vol. 5.
- [13] Any metric that depends only on the distance to the edge  $ds^2 = g_{xx}(y)dx^2 + 2g_{xy}(y)dxdy + g_{yy}(y)dy^2$  can be reduced to (1) by superposition of the in-plane displacement  $u(y) = -2 \int dy g_{xy}$  and  $v(y) = - \int dy (g_{yy} - 1)$ .
- [14] L. Landau and E. Lifshitz, *Theory of Elasticity* (Pergamon, Oxford, 1986).
- [15] A. E. Lobkovsky, S. Gentges, H. Li, D. Morse, and T. A. Witten, *Science* **270**, 1482 (1995).
- [16] M. Ben Amar and Y. Pomeau, *Proc. R. Soc. London, Ser. A* **453**, 729 (1997).
- [17] E. Cerda, S. Chaïeb, F. Melo, and L. Mahadevan, *Nature (London)* **401**, 46 (1999).
- [18] B. Roman and E. Sharon (private communication).
- [19] By tracking metastable solutions while letting their bending modulus go to zero, we found that their stretching energy converges to zero faster than  $h$ , therefore yielding embeddings in the limit  $h \rightarrow 0$ .